The Journal of Neuroscience, July 1993, 13(7): 2930–2938

RB and Cdc2 Expression in Brain: Correlations with ^{3}H-Thymidine Incorporation and Neurogenesis

Hirotaka J. Okano,[1,2] Donald W. Pfaff,[1] and Robert B. Gibbs[1]

[1]Laboratory of Neurobiology and Behavior, The Rockefeller University, New York, New York 10021 and [2]Graduate Studies Program, Jikei University School of Medicine, Tokyo, Japan

Expression of the cell cycle regulatory proteins RB and p34^{cdc2} was examined in the adult rat brain, with special emphasis on proliferation and neuronal differentiation in the hippocampal formation and olfactory bulb. RB-like immunoreactivity (RB-IR) was detected throughout the brain, with particularly intense staining observed in hippocampal pyramidal cells, pyriform cortex, and cerebellar Purkinje cells. Intense RB-IR and cdc2-IR were also detected in proliferating neuronal precursor cells in the subgranular region of the dentate gyrus and in the subependymal region extending from the anterior lateral ventricle into the olfactory bulb. Many of these cells developed into neurons as assessed by the expression of neuron-specific enolase (NSE) and, in the hipppocampal formation, the expression of Fos-IR following pentylenetetrazol-induced seizure activity. A good correlation was observed between the number of proliferating cells expressing intense nuclear RB-IR staining and the number of thymidine-labeled cells that had differentiated into functional hippocampal neurons. A substantial decrease in RB-IR during differentiation was also observed and occurred prior to the expression of NSE. The possibility that the loss of RB may be necessary for neuronal differentiation to proceed is discussed.

[Key words: retinoblastoma susceptibility gene, cellular proliferation, neural development, hippocampal formation, olfactory bulb]

Neurogenesis in the mammalian CNS is predominantly a prenatal event. Two exceptions are the hippocampal formation and olfactory bulb, where the majority of granule cells are produced during early postnatal life and continue to be produced well into adulthood (Kaplan and Hinds, 1977; Bayer, 1982; Bayer et al., 1982; Guéneau et al., 1982; Stanfield and Trice, 1988; Altman and Bayer, 1990). Relatively little is known about the mechanisms that regulate neurogenesis in brain. However, two proteins have recently been identified that appear to play pivotal roles in cell cycle regulation within all cell types examined thus far. RB, the retinoblastoma susceptibility gene, is one of a growing number of tumor suppressor genes. The protein product of the RB gene is a nuclear phosphoprotein that can bind and sequester transcription factors involved in cell cycle progression (Bagchi et al., 1991; Bandara and La Thangue, 1991; Bandara et al., 1991; Chellappan et al., 1991; Defeo-Jones et al., 1991; Kaelin et al., 1991) and whose absence or inactivation has been correlated with the release from cell cycle inhibition (Goodrich et al., 1991; Hara et al., 1991; Hatzfeld et al., 1991) and the development of a variety of neoplasms (Abramson et al., 1984; Friend et al., 1987; Harbour et al., 1988; Lee et al., 1988; T'Ang et al., 1988; Shew et al., 1989; Bookstein et al., 1990; Hensel et al., 1990; Horowitz et al., 1990; Ishikawa et al., 1991). In addition, recent studies have shown that transgenic mice that lack a functional RB gene are nonviable and exhibit extensive neuronal degeneration during middle embryonic stages (Clarke et al., 1992; Jacks et al., 1992; Lee et al., 1992), suggesting a critical role for RB during CNS development. The activity of RB is determined, at least in part, by its phosphorylation state with the underphosphorylated form associated with cell cycle inhibition (Buchkovich et al., 1989; Chen et al., 1989; Ludlow et al., 1990; Mihara et al., 1990; Goodrich et al., 1991). One kinase that has been implicated in the phosphorylation and inactivation of RB is the cell cycle–related kinase cdc2. Cdc2 (the p34^{cdc2} kinase) was originally described as the catalytic subunit of mitosis-promoting factor in frog oocytes as well as being essential to the initiation of mitosis in yeast (for reviews, see Dunphy and Newport, 1988; Lee and Nurse, 1988; Draetta, 1990; Nurse, 1990). Cdc2 in association with various cyclins has since been shown to play an essential role in the initiation of mitosis in a wide variety of eukaryotic cells from yeast to humans, as well as an essential role in the G_1 to S transition in yeast (Dunphy and Newport, 1988; Lee and Nurse, 1988; Draetta, 1990; Nurse, 1990). Like RB, the phosphorylation state of cdc2 oscillates during the cell cycle, with the hypophosphorylated form associated with the initiation of mitosis and commitment to divide (Draetta and Beach, 1988; Nurse, 1990). Cdc2 has also been shown to bind with and to catalyze the phosphorylation of RB (Lees et al., 1991; Lin et al., 1991). Studies indicate that both RB and cdc2 are expressed in brain (Bernards et al., 1989); however, there have been no studies localizing their expression to specific cell types or correlating their expression in brain with cellular proliferation. In the present study we have combined immunocytochemical techniques with autoradiographic detection of ^{3}H-thymidine (^{3}H-Thy) incorporation in order to characterize the expression of these cell cycle–related proteins as cells proliferate and differentiate into functional neurons. In this report we have focused on proliferating cells in the adult hippocampal formation and olfactory bulb since many of these cells are neuroblasts that have been

Received Nov. 13, 1992; revised Jan. 11, 1993; accepted Jan. 20, 1993.

We thank Dr. David Beach for generously supplying the mammalian p34^{cdc2} antibody, Dr. Michael Iadarolla for generously supplying the Fos antibody, and Dr. Sibylle Mittnadt for her advise and technical assistance during the course of this study. This work was supported by NIH Grant NS28896.

Correspondence should be addressed to Robert B. Gibbs at his present address: Department of Pharmacology and Therapeutics, 904 Salk Hall, University of Pittsburgh, Pittsburgh, PA 15261.

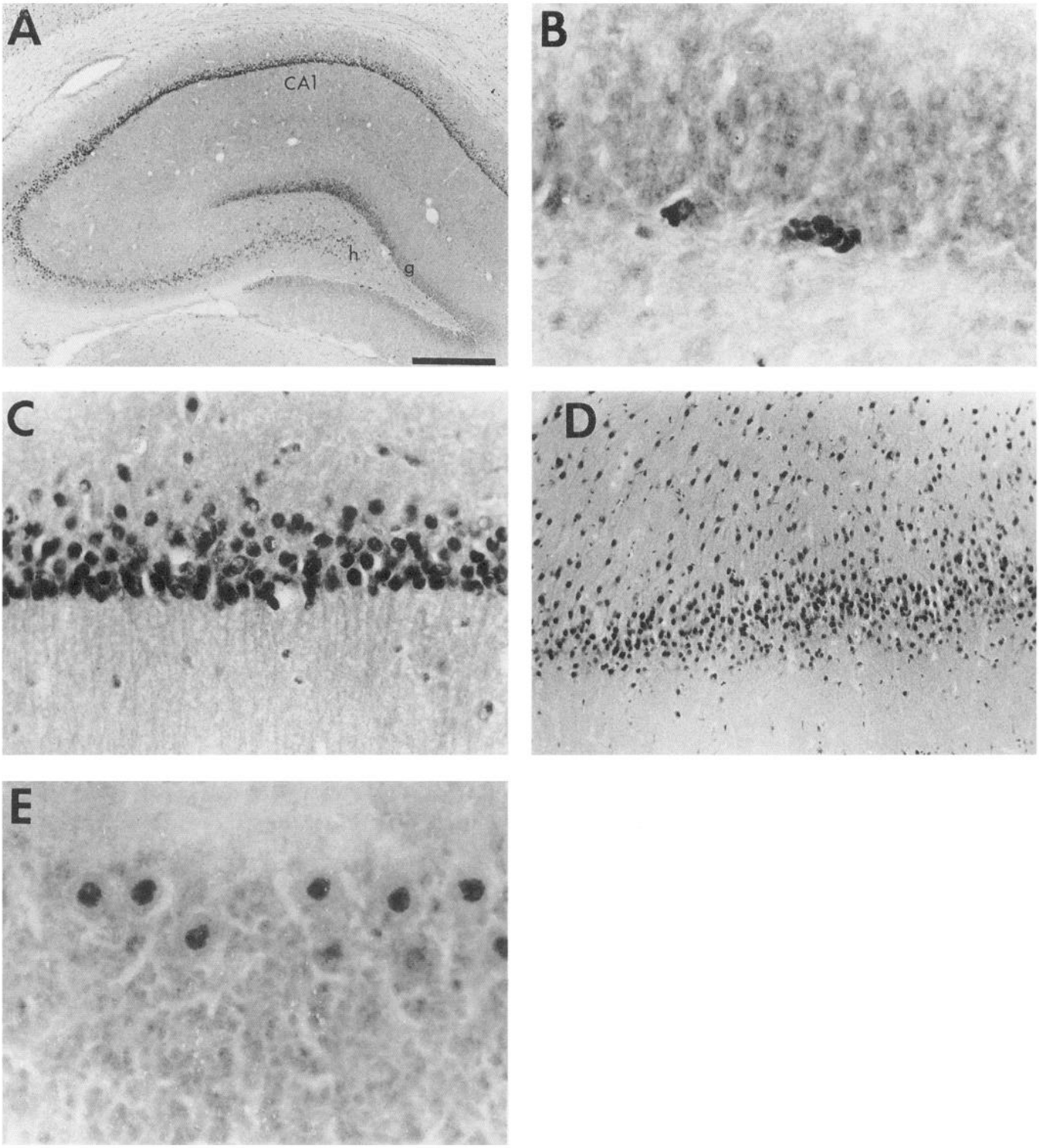

Figure 1. *A*, RB-IR cells in the hippocampal formation. Note that many hippocampal pyramidal cells (particularly in area CA1) as well as some hilar cells and some cells in the subgranular region of the dentate gyrus are intensely stained. *B*, Two clusters of intensely labeled RB-IR cells in the subgranular region of the dentate gyrus. *C*, Closer view of intense RB-IR staining in hippocampal CA1 pyramidal cells. Note that most of the staining is nuclear, but that some stain in the apical dendrites can also be observed. *D*, Intensely labeled RB-IR cells in the pyriform cortex. *E*, Intense RB-IR staining in the nuclei of cerebellar Purkinje cells. *g*, granule cell layer; *h*, hilus. Scale bar: *A*, 500 μm; *B*, *C*, and *E*, 30 μm; *D* 50 μm.

shown to give rise to granule cell neurons from early postnatal periods through adulthood (Kaplan and Hinds, 1977; Bayer, 1982; Bayer et al., 1982; Guéneau et al., 1982; Stanfield and Trice, 1988; Altman and Bayer, 1990; Gould et al., 1992).

Materials and Methods

Animal preparation and tissue processing. Thirty-one adult male Sprague–Dawley rats (180–200 gm) were used. All animals were treated and cared for in accordance with NIH and The Rockefeller University

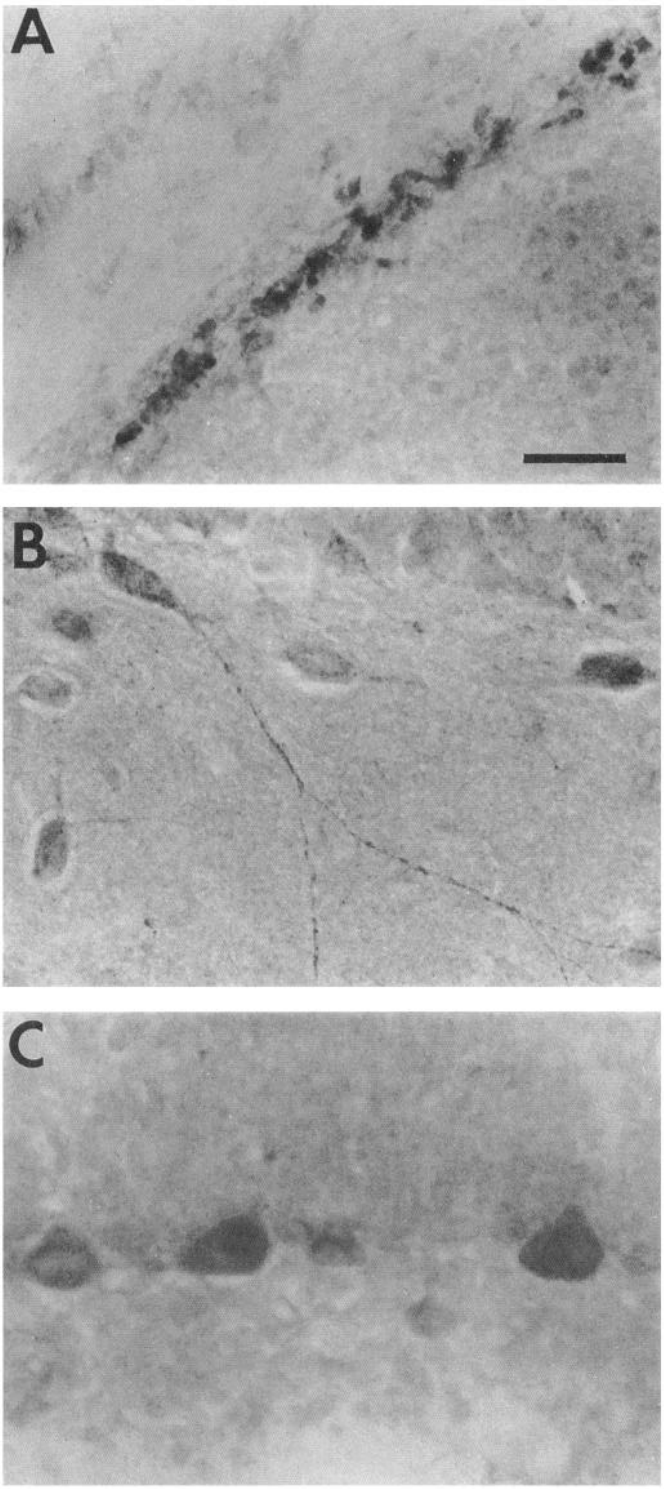

Table 1. Percentage of ^{3}H-Thy–labeled cells in the dentate gyrus expressing RB-, cdc2-, or NSE-IR at different times postinjection

Time	RB	cdc2	NSE
2 hr	80.5 ± 2.2	32.5 ± 2.8	0.3 ± 0.3
12 hr	58.8 ± 3.8	43.3 ± 1.6	0.6 ± 0.5
24 hr	40.5 ± 2.2	42.5 ± 3.1	0.9 ± 0.4
3 d	12.8 ± 5.1	11.0 ± 1.7	3.2 ± 0.3
1 wk	1.6 ± 0.5	1.7 ± 0.3	14.3 ± 1.6
4 wk	0.5 ± 0.3	0.2 ± 0.2	82.0 ± 2.1

guidelines. Animals received a single injection of ^{3}H-Thy (4 μCi/gm body weight, s.c.). At 2 hr (n = 4), 12 hr (n = 4), 24 hr (n = 4), 3 d (n = 3), 1 week (n = 4), and 4 weeks (n = 4) postinjection, animals were anesthetized with pentobarbital (50 mg/kg) and perfused with saline followed by 4% paraformaldehyde in 50 mM PBS. Brains were removed, postfixed with paraformaldehyde for 4 hr, and then placed in a 10% sucrose/PBS solution at 4°C overnight. Thirty-micrometer frozen sections were cut in the coronal plane through the hippocampal formation and cerebellum and in the sagittal plane through the olfactory bulb and anterior lateral ventricle. Adjacent series were processed for immunocytochemical detection of either RB (monoclonal antibody purchased from Pharmingen Pharmaceuticals and used at 4 μg/ml), mammalian cdc2 [rabbit anti-cdc2 (G6) raised against the C-terminal region of cdc2 generously provided by Dr. D. Beach and diluted 1:1000], neuron-specific enolase (NSE; rabbit anti-NSE purchased from Cambridge Pharmaceuticals and diluted 1:3000), or Fos and Fos-related antigens [rabbit anti-Fos raised against amino acids 127–152 (m-peptide) generously provided by Dr. M. Iadarolla and diluted 1:2000]. All antibodies were diluted in 50 mM PBS with 0.05% Triton X-100, 1% BSA, and 1% normal serum. Sections were incubated with primary antibody solution for 2–3 d at 4°C. To control for nonspecific binding, primary antibody either was omitted or was preadsorbed with 4 μg/ml of the appropriate antigen (a fragment of recombinant human RB, provided by Dr. Sibylle Mittnadt; NSE, Cambridge Pharmaceuticals; or m-peptide, provided by Dr. T. Curran). Antigen corresponding to the C-terminal region of cdc2 was not available. However, the cdc2 antibody used has been well characterized (Draetta and Beach, 1988), appears to be highly specific for cdc2, and does not recognize several cdc2-related kinases. Sections were then rinsed with PBS and incubated with the appropriate biotinylated secondary antibody (rat-adsorbed horse anti-mouse for the detection of RB and goat anti-rabbit for the detection of cdc2, NSE, or Fos) for 1 hr at room temperature. Visualization of antibody binding was accomplished using an avidin–biotin–HRP system with 3-3′-diaminobenzidine (0.5 mg/ml) and H_2O_2 (0.01%) added to the final reaction solution. Sections were mounted onto gelatin-coated slides and then dipped in Kodak NTB-3 radiographic emulsion. Autoradiograms were

←

Figure 2. Examples of cdc2-IR in brain. *A*, Cdc2-IR cells in the subependymal region adjacent to the anterior lateral ventricle and extending into the olfactory bulb. *B*, Cdc2-IR cells in the dentate hilus. Note the prominent cdc2-IR process. *C*, Cdc2-IR staining in Purkinje cells. Note that cdc2-IR is detected in both the nucleus and cytoplasm whereas RB-IR was detected only in the nucleus (compare with Fig. 1*E*). Scale bar, 30 μm.

→

Figure 3. Thymidine autoradiography combined with immunocytochemical detection of RB (*A*), cdc2 (*B*), NSE (*C, D*), and Fos (*E, F*) in the dentate gyrus. Thymidine-labeled cells are identified by clusters of dark silver grains overlying individual nuclei. *A*, Thymidine-labeled/RB-positive cells detected in the subgranular region 2 hr after receiving ^{3}H-Thy. Note the intense RB-like reaction product detected in the thymidine-labeled cells in contrast to the weak immunoreactive stain detected in the adjacent granule cell layer. *B*, Thymidine-labeled cdc2-positive (*large arrow*) and cdc2-negative (*small arrows*) cells detected in the subgranular region 2 hr after receiving ^{3}H-Thy. *C*, Thymidine-labeled/NSE-negative cells (*arrows*) detected in the subgranular region 2 hr after receiving ^{3}H-Thy. Note that adjacent cells in the granule cell layer are NSE positive and that NSE staining is exclusively cytoplasmic. *D*, Thymidine-labeled/NSE-positive cell (*arrow*) detected in the granule cell layer 4 weeks after receiving ^{3}H-Thy. *E*, Thymidine-labeled/Fos-negative cells detected in the subgranular region 3 d after receiving ^{3}H-Thy and 3 hr after pentylenetetrazol-induced seizure activity. Note the presence of many Fos-positive cells in the adjacent granule cell layer. *F*, Thymidine-labeled/Fos-positive cells detected in the granule cell layer 4 weeks after receiving ^{3}H-Thy and 3 hr after pentylenetetrazol-induced seizure activity. *g*, granule cell layer. Scale bar, 30 μm.

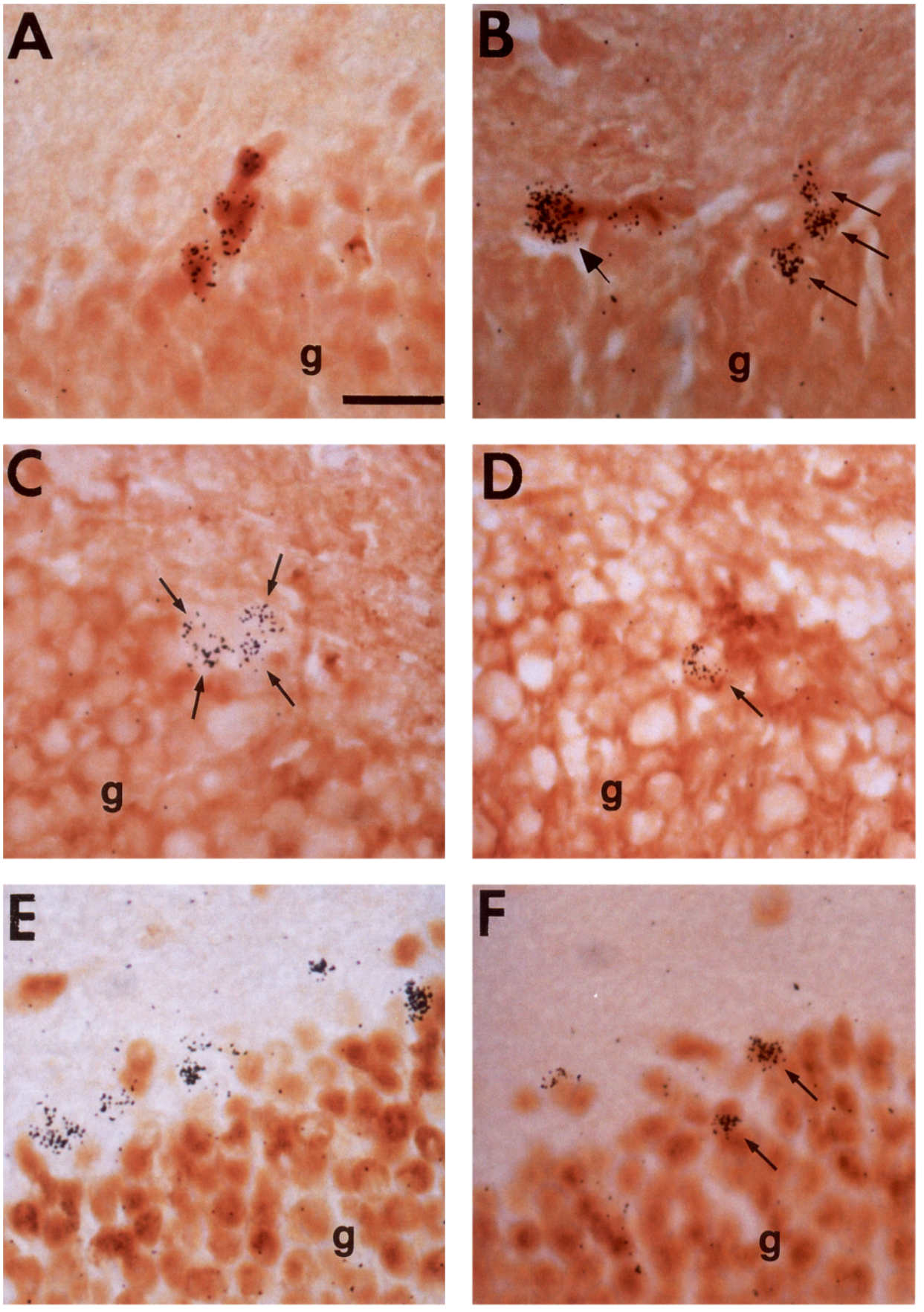
A
g
B
g
C
g
D
g
E
g
F
g

developed 7–10 d later. Slides were then dehydrated with ethanol, cleared in xylene, coverslipped with DePeX (Gurr, Inc.), and examined with a Zeiss photomicroscope.

Pentylenetetrazol-induced seizure activity. An additional eight animals received a single injection of pentylenetetrazol (50 mg/kg, i.p.) either 1 week ($n = 4$) or 4 weeks ($n = 4$) after receiving ^{3}H-Thy. Animals that displayed intense tonic/clonic seizure activity (two at 1 week and two at 4 weeks) were anesthetized and perfused 3 hr later and then processed for immunocytochemical detection of Fos-like immunoreactivity (Fos-IR) and autoradiography as described above.

Data analysis. Twelve equally spaced coronal sections through anterior and posterior regions of the hippocampal formation and two midsagittal sections through the olfactory bulb and anterior lateral ventricle were analyzed from each animal. The total numbers of ^{3}H-Thy–incorporating cells double labeled with RB-, cdc2-, NSE-, or Fos-IR in the subgranular region of the dentate gyrus, hippocampal CA4, and olfactory bulb were quantified. Note that, with respect to RB, only cells with intense nuclear RB-like staining (see Fig. 1*B*) were quantified. Since proliferating cells migrate rostrally within the periventricular region of the bulb, thymidine-labeled cells at different levels along the migratory path and within discrete cell layers including the internal granular layer, mitral cell layer, and glomerular layer were analyzed separately. This allowed us to correlate the detection of immunoreactivity with cellular migration and neuronal differentiation in the bulb.

Results

RB-IR was detected in neurons and glial cells throughout the brain, which is consistent with the relatively high levels of RB mRNA that have been detected (Bernards et al., 1989). Large regional differences in staining density were observed, with the most intense staining consistently detected in hippocampal CA1 pyramidal cells, pyriform cortex, and cerebellar Purkinje cells (Fig. 1). Significant staining was also observed in many other areas including the other hippocampal cell layers (Fig. 1*A*), the striatum, thalamus, hypothalamus, cerebral cortex, and amygdala (not shown). Indeed, few cells appeared to be completely devoid of RB-IR. All RB staining could be abolished by preadsorption of the antibody with a fragment of recombinant human RB (not shown). RB-IR was predominantly nuclear, although cytoplasmic staining was also observed, particularly in CA1 pyramidal cells, where nuclear staining was quite intense (Fig. 1*C*). Intensely stained RB-IR cells were also detected in the subgranular region of the dentate gyrus and along the subependymal layer of the anterior lateral ventricle extending into the olfactory bulb. In the dentate gyrus, these cells were organized in small, tightly packed groups or islands (Fig. 1*B*) from which individual cells would migrate into the granule cell layer and develop into mature granule cells (see below).

Cdc2-IR was also detected in brain, though not as ubiquitously as RB-IR. Cdc2-positive cells were detected in the hilus of the dentate gyrus (Fig. 2*B*) as well as in cerebellar Purkinje cells (Fig. 2*C*) and olfactory bulb mitral cells (not shown). As with RB, cdc2-IR cells were also detected in the subgranular region of the dentate gyrus (see below) and along the subependymal layer extending from the anterior lateral ventricle into the olfactory bulb (Fig. 2*A*). Note that Cdc2-IR staining was often both nuclear and cytoplasmic (see Fig. 2*B,C*), although cells with only nuclear or cytoplasmic staining were also observed.

By combining immunocytochemistry with autoradiography, we were able to correlate RB and cdc2 expression with cellular proliferation and to analyze changes in immunoreactivity as cells matured and differentiated into functioning neurons. As illustrated in Figure 1*B*, small groups (islands) of intense RB-IR cells were detected in the subgranular region of the dentate gyrus. Approximately three to five of these groups (three or four cells/group) were detected per section, and the distribution of these cells closely matched the distribution of neuronal precursor cells that have previously been described (Kaplan and Hinds, 1977; Bayer, 1982; Bayer et al., 1982; Guáneau et al., 1982; Altman and Bayer, 1990). When animals were killed 2 hr after receiving thymidine, 80.5% of the thymidine-incorporating cells detected in the subgranular region of the dentate gyrus displayed intense nuclear RB-IR staining (see Table 1, Fig. 3*A*). In contrast, only 32.5% were immunoreactive for cdc2 (Fig. 2*B*) and very few (0.3%) were immunoreactive for NSE (see Fig. 3*C*). In many cases the cdc2-IR staining was cytoplasmic and cdc2-IR processes were occasionally observed. By 12 hr postinjection the percentage of ^{3}H-Thy–labeled cells in the subgranular region showing intense RB-IR had decreased to 58.8% while the percentage double-labeled for cdc2-IR increased to 43.3% (Table 1). We assume that by this time the majority of ^{3}H-Thy–labeled cells had exited S-phase and progressed into G_2- or M-phase. This is supported by the finding that 12 hr later (24 hr postinjection) the number of ^{3}H-Thy–labeled cells detected in the subgranular region had doubled (from 107.8 ± 23.3 to 234.0 ± 63.1 cells/12 sections/animal), indicating that the labeled cells detected 2 hr postinjection had indeed divided. In addition, the percentage of ^{3}H-Thy–labeled cells at this time showing intense RB-IR had decreased further to 40.5% while the percentage double labeled for cdc2-IR remained essentially unchanged (Table 1).

As the recently divided cells matured, their expression of RB-, cdc2-, and NSE-IR continued to change (see Table 1). Within 1 week postinjection, only 1.6% and 1.7% of ^{3}H-Thy–labeled cells in the dentate gyrus showed intense RB-IR or cdc2-IR whereas 14.3% now stained for NSE. In addition, many ^{3}H-Thy–labeled cells displaying less RB-IR than adjacent granule cells were now observed (not shown). By 4 weeks postinjection, very few ^{3}H-Thy–labeled cells with intense RB- or cdc2-IR were detected, although many cells showed weak RB-IR staining comparable to surrounding granule cells. In addition, 82.0% of the thymidine-labeled cells were now immunoreactive for NSE (Fig. 3*D*), demonstrating that the majority of these cells had indeed differentiated into neurons.

To determine if the newly differentiated neurons were functional, we examined the expression of Fos-IR in response to pentylenetetrazole-induced seizure activity. In the absence of induced seizures, very few (<1%) ^{3}H-Thy–labeled cells in the dentate gyrus were immunoreactive for Fos-IR at any of the six time points examined. However, within 3 hr following seizure activity, an induction of Fos-IR within 21.0% (at 1 week post-thymidine injection) and 81.3% (at 4 weeks post-thymidine injection) of the ^{3}H-Thy–labeled cells detected in the granule cell layer was observed (Fig. 3*E,F*), suggesting that these cells had formed functional connections.

Thymidine-labeled cells were also consistently detected in the subependymal region of the olfactory bulb. As in previous reports (Altman, 1969; Rosselli-Austin and Altman, 1979; Bayer, 1983; Kishi, 1987), precursor cells originated in the subependymal layer of the anterior lateral ventricle. The proliferating cells then migrated along the subependymal layer (the migratory route; see Fig. 4*A*) into the bulb where they entered the internal granular layer and differentiated into neurons and glia.

When animals were killed 2 hr after thymidine injection, the majority (74.1%) of ^{3}H-Thy–labeled cells showed strong nuclear RB-IR staining and were located predominantly in the sube-

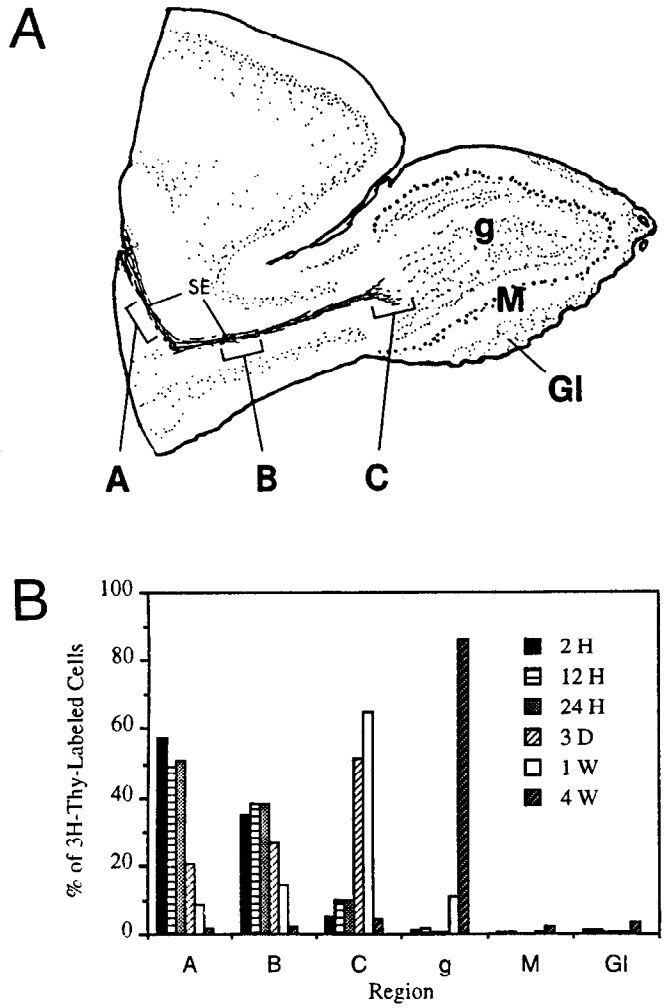

Figure 4. *A*, Drawing showing the subependymal layer (*SE*) through which proliferating cells migrate from the anterior lateral ventricle into the olfactory bulb and ultimately into the granular layer. *B*, Graph showing the percentage of thymidine-labeled cells detected at different positions along the migratory route 2 hr to 4 weeks after receiving ^{3}H-Thy. *g*, granular layer; *M*, mitral cell layer; *Gl*, glomerular layer.

pendymal layer near the anterior lateral ventricle (see Figs. 4, 5*A*). In contrast, only 30.4% were immunoreactive for cdc2 and none were immunoreactive for NSE (Table 2). Changes observed over time were comparable to those observed for ^{3}H-Thy–labeled cells detected in the subgranular region of the dentate gyrus. The percentage of ^{3}H-Thy–labeled cells showing intense RB-IR decreased to 41.2% and to 23.2% at 12 hr and 24 hr postinjection, respectively, by which time the number of ^{3}H-Thy–labeled cells detected had more than doubled (from 140.6 ± 6.7 to 340.1 ± 24.3 cells/2 sections/animal), indicating that the previously labeled cells had completed mitosis. During this time the percentage of ^{3}H-Thy–labeled cells immunoreactive for cdc2 also decreased to 21.0%. Note that little change was observed in the position of the cells along the migratory route during the first 24 hr postinjection (Fig. 4*B*).

As time passed and the cells migrated into the bulb, the percentage of ^{3}H-Thy–labeled cells showing RB- and cdc2-IR continued to decrease to where, by 1 week postinjection, only 1.5% and 1.6% were double labeled (see Table 2, Fig. 5*B*). By this time the majority of thymidine-incorporating cells were located

Table 2. Percentage of ^{3}H-Thy–labeled cells in the olfactory bulb expressing RB-, cdc2-, or NSE-IR at different times postinjection

Time	RB	cdc2	NSE
2 hr	74.1 ± 1.4	30.4 ± 1.7	0
12 hr	41.2 ± 4.7	25.0 ± 2.1	0
24 hr	23.2 ± 3.7	21.0 ± 4.3	0
3 d	5.2 ± 1.1	2.9 ± 0.2	0
1 wk	1.5 ± 0.2	1.6 ± 0.2	0
4 wk	0	0.3 ± 0.3	40.1 ± 3.9

at the anterior extent of the migratory route adjacent to the granule cell layer (Fig. 4*B*). Note, however, that relatively few cells had entered the granule cell layer and that none of the ^{3}H-Thy–labeled cells detected at this time were immunoreactive for NSE (Table 2, Fig. 5*C*). These data clearly show that RB- and cdc2-IR decrease prior to full neuronal differentiation. By 4 weeks postinjection, the majority (87%) of ^{3}H-Thy–labeled cells detected were located in the internal granular layer (Fig. 4*B*), none of which showed intense RB-IR staining and 40.1% of which were now immunoreactive for NSE (Table 2, Fig. 5*D*).

Discussion

The data demonstrate that RB- and cdc2-IR can be expressed both by proliferating and by nonproliferating cells in the adult brain. RB in particular was expressed throughout the brain, with very intense nuclear RB-IR staining observed in hippocampal pyramidal cells, cerebellar Purkinje cells, and pyriform cortex, as well as in neuroblasts located in the hippocampal formation and olfactory bulb. Cdc2-IR was much less ubiquitous and was detected in cerebellar Purkinje cells, olfactory bulb mitral cells, some hilar cells, and in some thymidine-labeled precursor cells. The data also indicate that the expression of RB and cdc2 changes dramatically as cells mature and differentiate into neurons. In particular, the number of thymidine-labeled cells expressing RB- or cdc2-IR decreased substantially to virtually undetectable levels within 1 week after thymidine injection. As cells matured, cdc2 continued to be undetectable whereas RB-IR increased to low but detectable levels comparable to the levels observed in adjacent granule cells.

The fact that only 32.5% and 30.4% of the thymidine-incorporating cells detected in the dentate gyrus and olfactory bulb, respectively, 2 hr postinjection displayed cdc2-IR suggests that cdc2 expression is not constant throughout the cell cycle and is not highly correlated with S-phase in these cells. This is consistent with recent findings that suggest that, in mammalian cells, one of several cdc2-related kinases, most notably the p33^{cdk2}, can functionally replace cdc2 during the G_1 to S transition (Elledge and Spottswood, 1991), possibly restricting cdc2's role in these cells to the G_2 to M transition and the commitment to divide (Tsai et al., 1991; Hamaguchi et al., 1992; Pagano et al., 1992). Since the antibody used in this study does not cross-react with cdk2 (Riabowol et al., 1989), the possibility that cdk2 or some other cdc2-related kinase is expressed in the nucleus of these cells during S-phase cannot be excluded.

A close correspondence was observed between the number of ^{3}H-Thy/RB-labeled cells detected 2 hr postinjection in the subgranular region of the dentate gyrus (80.5%) and the number of ^{3}H-Thy/NSE-labeled cells detected in the dentate granule cell layer 4 weeks later (82.0%), suggesting that most, if not all, of

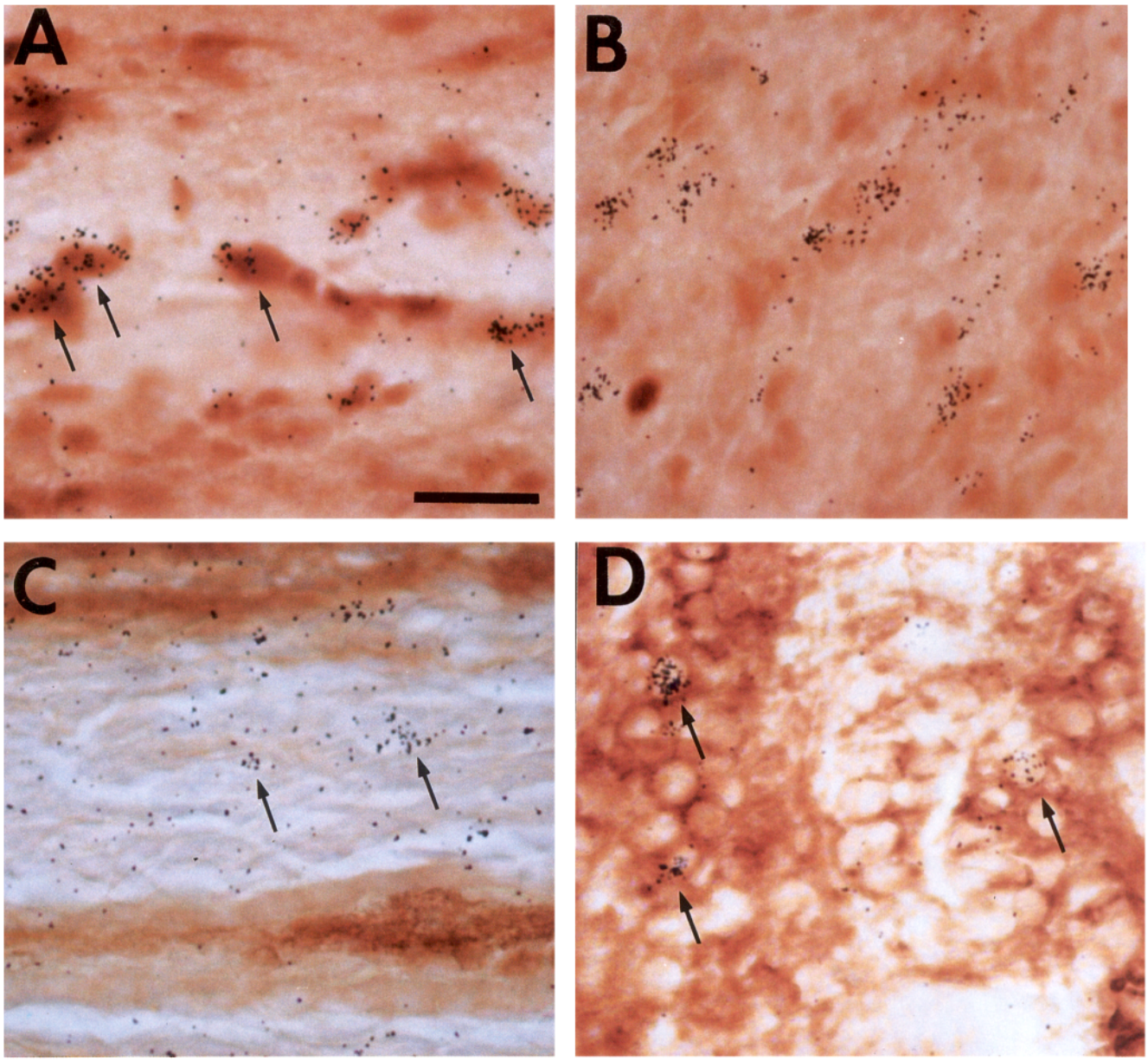

Figure 5. ^{3}H-Thy autoradiography combined with immunocytochemical detection of RB (*A, B*) or NSE (*C, D*) in the olfactory bulb. Thymidine-labeled cells are identified by clusters of dark silver grains overlying individual nuclei. *A*, Thymidine-labeled/RB-positive cells (*arrows*) detected in the subependymal layer 2 hr after receiving ^{3}H-Thy. Note the many RB-positive cells detected in this region of the subependymal layer. *B* and *C*, Thymidine-labeled cells detected in the anterior portion of the subependymal layer 1 week after receiving ^{3}H-Thy lack intense RB-IR (*B*) and NSE-IR (*C*) staining. Note the complete absence of NSE-like staining in the subependymal layer in *C* as contrasted with the NSE-positive staining detected on either side. *D*, Thymidine-labeled/NSE-positive cells (*arrows*) in the granular layer detected 4 weeks after receiving ^{3}H-Thy. Scale bar, 30 μm.

the ^{3}H-Thy/RB-labeled cells detected in this region differentiate into neurons. Similar results were observed in the subependymal region of the olfactory bulb, where 74.1% of the thymidine-labeled cells detected 2 hr postinjection showed intense nuclear RB-IR staining. In contrast, only 19.7% of the ^{3}H-Thy–labeled cells detected in the CA4 region of the dentate gyrus 2 hr post-injection showed intense nuclear RB-IR staining. Previous studies have identified small numbers of neuronal precursor cells located in CA4 that are thought to migrate to the subgranular region of the dentate gyrus (Bayer, 1982; Guéneau et al., 1982; Altman and Bayer, 1990). It has been suggested that the remaining thymidine-labeled cells in CA4 (the majority) represent a separate precursor population that remains in CA4 and gives rise to glia (Guéneau et al., 1982). Alternatively, these cells may constitute a pool of proliferating stem cells that migrate to the subgranular region and become "dividing transit cells" as defined by Potten and Loeffler (1990). In the present study, all ^{3}H-Thy–labeled cells detected in CA4 at 4 weeks postinjection were NSE negative. Likewise, of the small number of thymidine-incorporating cells detected elsewhere in the brain including the striatum, thalamus, and cortex, fewer than 10% displayed intense, nuclear RB-IR staining or were immunoreactive for NSE at any of the time points examined. Consequently, there appears to be a good correlation in these structures between intense

nuclear RB-IR staining during S-phase and subsequent neuronal differentiation.

Other evidence that RB plays a role during cellular differentiation has been reported. A correlation was recently observed between RB-IR staining and cellular differentiation/maturation in embryonic SCID mouse tissues (Szekely et al., 1992). Yen et al. (1992) have reported that terminal differentiation of HL-60 cells (a human promyelocytic leukemia cell line) is preceded by a reduction in the cellular content of RB, with failure to differentiate correlated with an insufficient reduction of RB. Likewise, a correlation between the inactivation of RB and the pathogenesis of lung tumors expressing neuronal or neuroendocrine phenotypes has been reported (Harbour et al., 1988). Evidence that RB plays a critical role during neuronal differentiation is also supported by recent findings showing that transgenic mice that lack a functional RB gene display severe CNS pathology and ectopic mitoses beginning in middle (embryonic days 10–11), but not early, embryonic development (Clarke et al., 1992; Jacks et al., 1992; Lee et al., 1992).

The function of RB in adult, differentiated CNS neurons is currently unclear. Many mitogenic growth factors, including epidermal growth factor, fibroblast growth factor, and insulin-like growth factors, are present in brain. One possibility is that constitutive expression of RB by CNS neurons is necessary to prevent growth factors from stimulating differentiated CNS neurons to divide. Another possibility is that RB actively regulates transcriptional activity associated with neuronal function. Many studies point to RB as a regulator of transcriptional activity via binding to intracellular factors such as E2F, c-myc, N-myc, and Fos (Bagchi et al., 1991; Bandara and La Thangue, 1991; Bandara et al., 1991; Chellappan et al., 1991; Defeo-Jones et al., 1991; Kaelin et al., 1991; Rustgi et al., 1991). In particular, the ability for the underphosphorylated form of RB to bind and sequester the transcription factor E2F has been strongly correlated with RB's ability to inhibit cell cycle progression (Bandara and La Thangue, 1991; Bandara et al., 1991; Chellappan et al., 1991; Chittenden et al., 1991). One recent study detected high levels of E2F mRNA in the adult brain relative to other tissues (Helin et al., 1992). The specific cells expressing E2F have not yet been identified; however, one possibility is that RB serves to regulate E2F activity in adult CNS neurons.

RB can also bind directly with DNA (Lee et al., 1987; Wang et al., 1990) and has been shown to regulate transcription from a variety of promoters including c-*fos*, c-*myc*, transforming growth factor β1 and insulin-like growth factor II (Pietenpol et al., 1990; Robbins et al., 1990; Kim et al., 1991, 1992). Most of these factors have been detected in the adult and developing CNS, where they have been postulated to play an important role in the transduction of extracellular signals associated with neural activation, synaptic plasticity, and growth (Adamson, 1987; Sudol, 1988). RB has also been shown to repress c-*fos* expression and AP-1 transcriptional activity in 3T3 cells (Robbins et al., 1990). Likewise, RB may regulate AP1 activity in neurons. We find it noteworthy that neurons that stained most intensely for RB-IR (i.e., CA1 pyramidal cells, pyriform cortex, and cerebellar Purkinje cells) have been demonstrated to be highly susceptible to neuronal loss following ischemia (Pulsinelli et al., 1982; Smith et al., 1984). Yen and coworkers have recently proposed that RB serves as a "status quo" gene whose function is to sustain a "developmentally ordained" state of proliferation or differentiation and that a change in RB expression indicates a change in the developmental or functional state of the cell (Yen et al., 1991, 1992). The possibility that RB may be serving a similar function in brain is intriguing and merits further study.

References

Abramson DH, Ellsworth RM, Kitchin D, Tung G (1984) Second nonocular tumors in retinoblastoma survivors. Ophthalmology 91: 1351–1355.

Adamson ED (1987) Oncogenes in development. Development 99: 449–471.

Altman J (1969) Autoradiographic and histologic studies of postnatal neurogenesis. IV. Cell proliferation and migration in the anterior forebrain, with special reference to persisting neurogenesis in the olfactory bulb. J Comp Neurol 137:433–458.

Altman J, Bayer SA (1990) Migration and distribution of two populations of hippocampal granule cell precursors during the perinatal and postnatal periods. J Comp Neurol 301:365–381.

Bagchi S, Weinmann R, Raychaudhuri P (1991) The retinoblastoma protein copurifies with E2F-I, and E1a-regulated inhibitor of the transcription factor E2F. Cell 65:1063–1072.

Bandara LR, La Thangue NB (1991) Adenovirus E1A prevents the retinoblastoma gene product from complexing with a cellular transcription factor. Nature 351:494–497.

Bandara LR, Adamczewski JP, Hunt T, La Thangue NB (1991) Cyclin A and the retinoblastoma gene product complex with a common transcription factor. Nature 352:249–251.

Bayer SA (1982) Changes in the total number of dentate granule cells in juvenile and adult rats: a correlated volumetric and ^{3}H-thymidine autoradiographic study. Exp Brain Res 46:315–323.

Bayer SA (1983) ^{3}H-thymidine-radioautographic studies pf neurogenesis in the rat olfactory bulb. Exp Brain Res 50:329–340.

Bayer SA, Yackel JW, Puri PS (1982) Neurons in the rat dentate gyrus granular layer substantially increase during juvenile and adult life. Science 216:890–892.

Bernards R, Bernards R, Schackleford GM, Gerber MR, Horowitz JM, Friend SH, Schartl M, Bogenmann E, Rapaport JM, McGee T, Dryja TP, Weinberg RA (1989) Structure and expression of the murine retinoblastoma gene and characterization of its encoded protein. Proc Natl Acad Sci USA 86:6474–6478.

Bookstein R, Shew J-Y, Chen P-L, Lee W-H (1990) Suppression of tumorigenicity of human prostate carcinoma cells by replacing mutated RB gene. Science 247:712–715.

Buchkovich K, Duffy LA, Harlow E (1989) The retinoblastoma protein is phosphorylated during specific phases of the cell cycle. Cell 58: 1097–1105.

Chellappan SP, Hiebert S, Mudryj M, Horowitz JM, Nevins JR (1991) The E2F transcription factor is a cellular target for the RB protein. Cell 65:1053–1061.

Chen P-L, Scully P, Shew J-Y, Wang YJ, Lee W-H (1989) Phosphorylation of the retinoblastoma gene product is modulated during the cell cycle and cellular differentiation. Cell 58:1193–1198.

Chittenden T, Livingston DM, Kaelin WGJ (1991) The T/E1A-binding domain of the retinoblastoma product can interact selectively with a sequence-specific DNA-binding protein. Cell 65:1073–1082.

Clarke AR, Maandag ER, van Roon M, van der Lugt NMT, van der Valk M, Hooper ML, Berns A, te Riele H (1992) Requirement for a functional Rb-1 gene in murine development. Nature 359:328–330.

Defeo-Jones D, Huang PS, Jones RE, Haskell KM, Vuocolo GA, Hanobik MG, Huber HE, Oliff A (1991) Cloning of cDNAs for cellular proteins that bind to the retinoblastoma gene product. Nature 352: 251–254.

Draetta G (1990) Cell cycle control in eukaryotes: molecular mechanisms of cdc2 activation. Trends Biochem Sci 15:378–382.

Draetta G, Beach D (1988) Activation of *cdc2* protein kinase during mitosis in human cells: cell cycle-dependent phosphorylation and subunit rearrangement. Cell 54:17–26.

Dunphy WG, Newport JW (1988) Unraveling of mitotic control mechanisms. Cell 55:925–928.

Elledge SJ, Spottswood MR (1991) A new human p34 protein kinase, CDK2, identified by complementation of a cdc28 mutation in *Saccharomyces cerevisiae*, is a homolog of *Xenopus* Eg1. EMBO J 10: 2653–2659.

Friend SH, Horowitz JM, Gerber MR, Wang X-F, Bogenman E, Li FP, Weinberg RA (1987) Deletions of a DNA sequence in retinoblas-

tomas and mesenchymal tumors: organization of the sequence and its encoded protein. Proc Natl Acad Sci USA 84:9059–9063.
Goodrich DW, Wang NP, Qian Y-W, Lee EY-HP, Lee W-H (1991) The retinoblastoma gene product regulates progression through G1 phase of the cell cycle. Cell 67:293–302.
Gould E, Cameron HA, Daniels DC, Woolley CS, McEwen BS (1992) Adrenal hormones suppress cell division in the adult rat dentate gyrus. J Neurosci. 12:3642–3650.
Guéneau G, Privat A, Drouet J, Court L (1982) Subgranular zone of the dentate gyrus of young rabbits as a secondary matrix. Dev Neurosci 5:345–358.
Hamaguchi JR, Tobey RA, Pines J, Crissman HA, Hunter T, Bradbury EM (1992) Requirement for $p34^{cdc2}$ kinase is restricted to mitosis in the mammalian cdc2 mutant FT210. J Cell Biol 115:1041–1053.
Hara E, Tsurui H, Shinozaki A, Nakada S, Oda K (1991) Cooperative effect of antisense-Rb and antisense-p53 oligomers on the extension of life span in human diploid fibroblasts. Biochem Biophys Res Commun 179:528–534.
Harbour JW, Lai S-L, Whang-Peng J, Gazdar AF, Minna D, Kaye FJ (1988) Abnormalities in structure and expression of the human retinoblastoma gene in SCLC. Science 241:353–357.
Hatzfeld J, Li M-L, Brown EL, Sookdeo H, Levesque J-P, O'Toole T, Gurney C, Clark SC, Hatzfeld A (1991) Release of early human hematopoietic progenitors from quiescence by antisense transforming growth factor β1 or Rb oligonucleotides. J Exp Med 174:925–929.
Helin K, Lees JA, Vidal M, Dyson N, Harlow E, Fattaey A (1992) A cDNA encoding a pRN-binding protein with properties of the transcription factor E2F. Cell 70:337–350.
Hensel CH, Hsieh CL, Gazdar AF, Johnson BE, Sakaguchi AY, Naylor SL, Lee W-HP (1990) Altered structure and expression of the human retinoblastoma susceptibility gene in small cell lung cancer. Cancer Res 50:3067–3072.
Horowitz JM, Park S-H, Bogenmann E, Cheng J-C, Yandell DW, Kaye FJ, Minna JD, Dryja TP, Weinberg RA (1990) Frequent inactivation of the retinoblastoma anti-oncogene is restricted to a subset of human tumor cells. Proc Natl Acad Sci USA 87:2775–2779.
Ishikawa J, Xu H-J, Hu S-X, Yandell DW, Maeda S, Kamidono S, Benedict WF, Takahashi R (1991) Inactivation of the retinoblastoma gene in human bladder renal cell carcinomas. Cancer Res 51: 5736–5743.
Jacks T, Fazeli A, Schmitt EM, Bronson RT, Goodell MA, Weinberg RA (1992) Effects of an Rb mutation in the mouse. Nature 359: 295–300.
Kaelin WGJJ, Pallas DC, DeCaprio JA, Kaye FJ, Livingston DM (1991) Identification of cellular proteins that can interact specifically with the T/E1A-binding region of the retinoblastoma gene product. Cell 64:521–532.
Kaplan MS, Hinds JW (1977) Neurogenesis in the adult rat. Electron microscopic analysis of light radioautographs. Science 197:1092–1094.
Kim S-J, Lee H-D, Robbins PD, Busam K, Sporn MB, Roberts AB (1991) Regulation of transforming growth factor β1 gene expression by the product of the retinoblastoma susceptibility gene. Proc Natl Acad Sci USA 88:3052–3056.
Kim S-J, Onwuta US, Lee YI, Li R, Botchan MR, Robbins PD (1992) The retinoblastoma gene product regulates Sp1-mediated transcription. Mol Cell Biol 12:2455–2463.
Kishi K (1987) Golgi studies on the development of granule cells of the rat olfactory bulb with reference to migration in the subependymal layer. J Comp Neurol 258:112–124.
Lee EY-HP, To H, Shew J-Y, Bookstein R, Scully P, Lee W-H (1988) Inactivation of the retinoblastoma susceptibility gene in human breast cancers. Science 241:218–221.
Lee EY-HP, Chang C-Y, Hu N, Wang Y-CJ, Lai C-C, Herrup K, Lee W-H, Bradley A (1992) Mice deficient for Rb are nonviable and show defects in neurogenesis and haematopoiesis. Nature 359:288–294.
Lee M, Nurse P (1988) Cell cycle control genes in fission yeast and mammalian cells. Trends Genet 4:287–289.
Lee W-H, Shew J-Y, Hong F, Sery T, Donoso LA, Young L-J, Bookstein R, Lee WY-HP (1987) The retinoblastoma susceptibility gene product is a nuclear phosphoprotein associated with DNA binding activity. Nature 329:642–645.
Lees JA, Buchkovich KJ, Marshak DR, Anderson CW, Harlow E (1991) The retinoblastoma protein is phosphorylated on multiple sites by human cdc2. EMBO J 10:4279–4290.
Lin BT-Y, Gruenwald S, Morla AO, Lee W-H, Wang JYJ (1991) Retinoblastoma cancer suppressor gene product is a substrate of the cell cycle regulator cdc2 kinase. EMBO J 10:857–864.
Ludlow JW, Shon JS, Pipas JM, Livingston DM, DeCaprio JA (1990) The retinoblastoma susceptibility gene product undergoes cell cycle-dependent dephosphorylation and binding to and release from SV40 large T. Cell 60:387–396.
Mihara K, Cao X-R, Yen A, Chandler S, Driscoll B, Murphree AL, T'Ang A, Fung Y-KT (1990) Cell cycle-dependent regulation of phosphorylation of the human retinoblastoma gene product. Science 246:1300–1303.
Nurse P (1990) Universal control mechanism regulating onset of M-phase. Nature 344:503–508.
Pagano M, Draetta G, Jansen-Dürr P (1992) Association of cdk2 kinase with the transcription factor E2F during S phase. Science 255: 1144–1147.
Pietenpol JA, Stein RW, Moran E, Yaciuk P, Schlegel R, Lyons RM, Pittelkow MR, Munger K, Howley PM, Moses HL (1990) TGF-β1 inhibition of c-myc transcription and growth in keratinocytes is abrogated by viral transforming proteins with pRB binding domains. Cell 61:777–785.
Potten CS, Loeffler M (1990) Stem cells: attributes, cycles, spirals, pitfalls and uncertainties. Lesson for and from the crypts. Development 110:1001–1020.
Pulsinelli WA, Brierley JB, Plum F (1982) Temporal profile of neuronal damage in a model of transient forebrain ischemia. Ann Neurol 11:491–498.
Riabowol K, Draetta G, Brizuela L, Vendre D, Beach D (1989) The cdc2 kinase is a nuclear protein that is essential for mitosis in mammalian cells. Cell 57:393–401.
Robbins PD, Horowitz JM, Mulligan RC (1990) Negative regulation of human c-fos expression by the retinoblastoma gene product. Nature 346:668–671.
Rosselli-Austin L, Altman J (1979) The postnatal development of the main olfactory bulb of the rat. J Dev Physiol 1:295–313.
Rustgi AK, Dyson N, Bernards R (1991) Amino-terminal domains of c-myc and N-myc proteins mediate binding to the retinoblastoma gene product. Nature 352:541–544.
Shew J-Y, Ling N, Yang X, Fodstad O, Lee W-H (1989) Antibodies detecting abnormalities of the retinoblastoma susceptibility gene product (pp110RB) in osteosarcomas and synovial sarcomas. Oncogene Res 1:205–214.
Smith M-L, Auer RN, Siesjö BK (1984) The density and distribution of ischemic brain injury in the rat following 2–10 minutes of forebrain ischemia. Acta Neuropathol (Berl) 64:319–332.
Stanfield BB, Trice JE (1988) Evidence that granule cells generated in the dentate gyrus of adult rats extend axonal projections. Exp Brain Res 72:399–406.
Sudol M (1988) Expression of proto-oncogenes in neural tissues. Brain Res Rev 13:391–403.
Szekely L, Jiang W-Q, Bulic-Jakus F, Rosen A, Ringertz N, Klein G, Wiman KG (1992) Cell type and differentiation dependent heterogeneity in retinoblastoma protein expression in SCID mouse fetuses. Cell Growth Diff 3:149–156.
T'Ang A, Varley J, Chakraborty S, Murphree AL, Fung YK (1988) Structural rearrangement of the retinoblastoma gene in human breast carcinoma. Science 242:263–266.
Tsai L-H, Harlow E, Meyerson M (1991) Isolation of the human *cdk2* gene that encodes the cyclin A- and adenovirus E1A-associated p33 kinase. Nature 353:174–177.
Wang N-P, Chen P-L, Huang S, Donoso LA, Lee W-H, Lee EY-HP (1990) DNA-binding activity of retinoblastoma protein is intrinsic to its carboxyl-terminal region. Cell Growth Diff 1:233–239.
Yen A, Chandler S, Sturzenegger-Varvayanis S (1991) Regulated expression of the RB "tumor suppressor gene" in normal lymphocyte mitogenesis: elevated expression in transformed leukocytes and role as a "status quo" gene. Exp Cell Res 192:289–297.
Yen A, Chandler S, Forbes ME, Fung Y-K, T'Ang A, Pearson R (1992) Coupled down-regulation of the RB retinoblastoma and c-myc genes antecedes cell differentiation: possible role of RB as a "status quo" gene. Eur J Cell Biol 57:210–221.